

Red-shifted H₂O emission in NGC 3079: More evidence for a pc-scale circumnuclear torus?*

Y. Hagiwara^{1,2}, C. Henkel¹, W. A. Sherwood¹, and W. A. Baan²

¹ Max-Planck-Institut für Radioastronomie, Auf dem Hügel 69, 53121 Bonn, Germany

² Westerbork Observatory, PO Box 2, 7990 AA Dwingeloo, The Netherlands

Received 23 January 2002 / Accepted 2 April 2002

Abstract. Using the Effelsberg 100-m telescope, sensitive measurements of the H₂O megamaser in NGC 3079 are presented. During 2000–2001, “high velocity” features are seen that are red-shifted up to 225 km s⁻¹ with respect to the systemic velocity of the galaxy ($V_{\text{LSR}} \sim 1120 \text{ km s}^{-1}$). Symmetrically bracketing the systemic velocity, the H₂O emission covers a velocity range of $\sim 450 \text{ km s}^{-1}$ with only one potential narrow gap ($\sim 20 \text{ km s}^{-1}$) near the systemic velocity itself. Velocity drifts of individual components are not convincingly detected. It is shown that the presence of red-shifted emission and the absence of detectable velocity drifts are not inconsistent with the existence of a rotating circumnuclear maser disk at the very center of the galaxy. Significant differences in the overall line profile compared to NGC 4258 and a complex morphology of the radio continuum leave, however, space for scepticism.

Key words. galaxies: active – galaxies: individual: NGC 3079 – galaxies: ISM – galaxies: nuclei – radio lines: galaxies

1. Introduction

Recent single-dish and VLBI observations of luminous H₂O megamasers have been motivated by the discovery of an edge-on Keplerian sub-pc scale maser disk enshrouding a compact supermassive object at the nucleus of the LINER galaxy NGC 4258 (e.g. Nakai et al. 1993, 1995; Haschick et al. 1994; Greenhill et al. 1995; Miyoshi et al. 1995; Herrnstein et al. 1999). Circumnuclear disk structures traced by H₂O are also seen towards NGC 1068, NGC 4945, and the Circinus galaxy (e.g. Gallimore et al. 2001; Greenhill et al. 1997, 2000). H₂O megamasers therefore provide a unique probe to study the kinematics and the dynamical structure of the innermost regions of active galactic nuclei.

For the LINER or Seyfert 2 galaxy NGC 3079 (see Sawada-Satoh et al. 2000) that contains one of the most luminous H₂O megamasers known to date (e.g. Henkel et al. 1984; Haschick & Baan 1985; Haschick et al. 1990), arguments in favor of a circumnuclear disk have been less compelling. While the known maser components arise in the inner few parsecs of the galaxy, they do not align at right angles to the radio jet(s), almost all the detected emission is blue-shifted relative to the systemic velocity, and any velocity drift of individual H₂O features must be small

Send offprint requests to: Y. Hagiwara, Dwingeloo

* Based on observations with the 100-m telescope of the MPIfR (Max-Planck-Institut für Radioastronomie) at Effelsberg.

($\lesssim 4.0 \text{ km s}^{-1} \text{ yr}^{-1}$; Nakai et al. 1995; Baan & Haschick 1996; Trotter et al. 1998; Satoh et al. 1999; Sawada-Satoh et al. 2000).

In this letter we therefore report single-dish observations of the 22 GHz water vapor line from NGC 3079, (1) to look for the missing red-shifted velocity components and (2) to search for velocity drifts in the near systemic features that would indicate centripetal acceleration in a rotating circumnuclear disk.

2. Observations

Observations of the $J_{K_a K_c} = 6_{16} - 5_{23}$ H₂O maser line (rest frequency: 22.23508 GHz) were made with the MPIfR 100-m radio telescope at Effelsberg between February 1994 and December 2001. Until 1998, a single channel *K*-band maser receiver was employed in a position switching mode with a system temperature of $T_{\text{sys}} \sim 225 \text{ K}$ on a main beam brightness temperature (T_{mb}) scale. An autocorrelator provided bandwidths of 50, 25 or 12.5 MHz with 1024 spectral channels, yielding channel spacings of 0.66, 0.33 or 0.16 km s⁻¹. Since 2000, we used a dual channel *K*-band HEMT receiver in a dual beam switching mode with a beam throw of 2' and a switching frequency of 1 Hz. After averaging the two orthogonally polarized signals, $T_{\text{sys}} \sim 180 \text{ K}$. Four autocorrelator backends were employed for each receiver channel. Each spectrum had a bandwidth of 40 MHz and 512 channels, yielding a channel spacing of 1.05 km s⁻¹.

Table 1. Effelsberg 100-m observations log^{a)}.

Epoch			Epoch		
1994	Feb.	9	2000	Mar.	18
1995	Sep.	16–17	2000	Oct.	14
1996	Sep.	21–23	2000	Dec.	21
1997	Apr.	5–6	2000	Mar.	13
1997	Nov.	5	2001	Apr.	22
1998	Feb.	1	2001	May	9
1998	May	8	2001	Dec.	5
1998	Jun.	27			
1998	Aug.	1			

^{a)} Several tunings and bandwidths were employed during most epochs. As a consequence, noise levels and channel spacings are not uniform across the observed velocity ranges. 1σ noise levels vary from 200 mJy (channel spacing 1.32 km s^{-1}) in September 1996 to 7 mJy (channel spacing 1.05 km s^{-1}) in December 2001. Velocity resolution $\sim 1.25 \times$ channel spacing. For direct access to 64 flux calibrated spectra, contact chenkel@mpifr-bonn.mpg.de.

Amplitude calibration was based on measurements of the 22 GHz continuum flux of 3C 286 (see Baars et al. 1977; Ott et al. 1994). Pointing measurements toward nearby sources (in most cases DA 251) were made once per hour. The resultant pointing accuracy was $< 8''$, that should be compared with the full width to half power beam size of $40''$. Calibration uncertainties are estimated to be $\pm 15\%$.

3. Results

H₂O spectra were taken during 16 epochs (Table 1; no changes in the maser profiles were seen *within* any of these observing periods). Several H₂O features could be traced over the entire monitoring period. The most prominent component, detected at $\sim 956 \text{ km s}^{-1}$, showed a peak flux density of 2.5–4.5 Jy. While the peak velocity is observed to drift from about 955.0 to 956.8 km s^{-1} (estimated error of individual measurements: 0.3 km s^{-1}), this drift is not systematic and appears to be caused by a multitude of individual, variable subcomponents. During times with lower peak velocity, the profile tends to show a “shoulder” at the high velocity wing of the line (e.g., on Nov. 5, 1997 and Feb. 1, 1998) and vice versa (Dec. 21, 2000, and Apr. 22, 2001). Notable were two flares of more red-shifted components that exceeded 2 Jy: The 979 km s^{-1} component with 0.7 Jy during Feb. 1994 to Apr. 1997 (see Nakai et al. 1995 for earlier spectra) reached 0.9 Jy in Nov. 1997, 1.5 Jy in Feb. 1998, and 2.2 Jy in May 1998 (Fig. 1a); it then decreased to 1.8 Jy in June 1998, 1.25 Jy in Aug. 1998, and 0.35 Jy since Oct. 2000. The 1017 km s^{-1} velocity component, observed between Sep. 1996 and Nov. 1997 at 0.1–0.5 Jy, reached a peak flux density of 2.5 Jy in Mar. 2000 (Fig. 1b); flux densities decreased to 1.0 Jy in Oct. 2000 and to 0.1 Jy

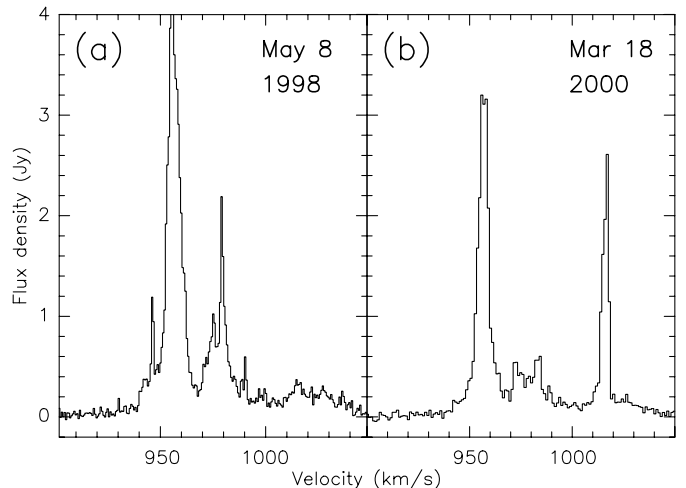


Fig. 1. The **a)** 979 and **b)** 1017 km s^{-1} features flaring beyond the 2 Jy level (channel spacings: 0.66 and 1.05 km s^{-1}). Velocity scale throughout the paper: Local Standard of Rest (LSR), following the radio astronomical definition of velocity (see e.g. Trotter et al. 1998). $V_{\text{LSR}} = V_{\text{HEL}} + 3.23 \text{ km s}^{-1}$.

in May 2001. Emission near the systemic velocity of the galaxy ($1080 \text{ km s}^{-1} < V_{\text{LSR}} < 1160 \text{ km s}^{-1}$) remained faint and not a single narrow velocity component could be traced during several consecutive observing epochs.

Figure 2 shows a spectrum of near systemic ($V_{\text{sys}} \sim 1120 \text{ km s}^{-1}$) and red-shifted ($V > V_{\text{sys}}$) features that were detected since March 2000. More than 10 distinct narrow components appear at velocities in excess of 1100 km s^{-1} (Table 2). We conclude that the H₂O maser emission extends over a radial velocity range of $\sim 450 \text{ km s}^{-1}$. The integrated luminosity of the previously known blue-shifted components remains approximately constant. This may also hold for the systemic and red-shifted features shown in Fig. 2. A detection of these prior to 2000 would have been difficult in view of technical improvements that occurred at Effelsberg in 1999. Sensitivity also limits the studies by Nakai et al. (1995; we do not confirm the weak 764 and 791 km s^{-1} components) and Baan & Haschick (1996). However, the 1123 and 1190 km s^{-1} components observed by Trotter et al. (1998) in Jan. 1995, the flaring 1192 km s^{-1} feature ($\sim 0.4 \text{ Jy}$) detected by Nakai et al. (1995) in Apr.–May 1995, and a 1201 km s^{-1} feature detected by us in Sep. 1995 (Fig. 3) indicate the presence of isolated red-shifted maser features as early as half a dozen years ago.

4. Discussion

In NGC 4258, Nakai et al. (1993) detected red- and blue-shifted H₂O “satellites” symmetrically displaced by approximately $\pm 900 \text{ km s}^{-1}$ from the systemic velocity. This suggested the presence of a circumnuclear disk that was later confirmed (see Sect. 1). Is the discovery of a multitude of near systemic and red-shifted features in NGC 3079 also hinting at a circumnuclear disk? Emission is seen at least between 928 and 1352 km s^{-1} (Fig. 3).

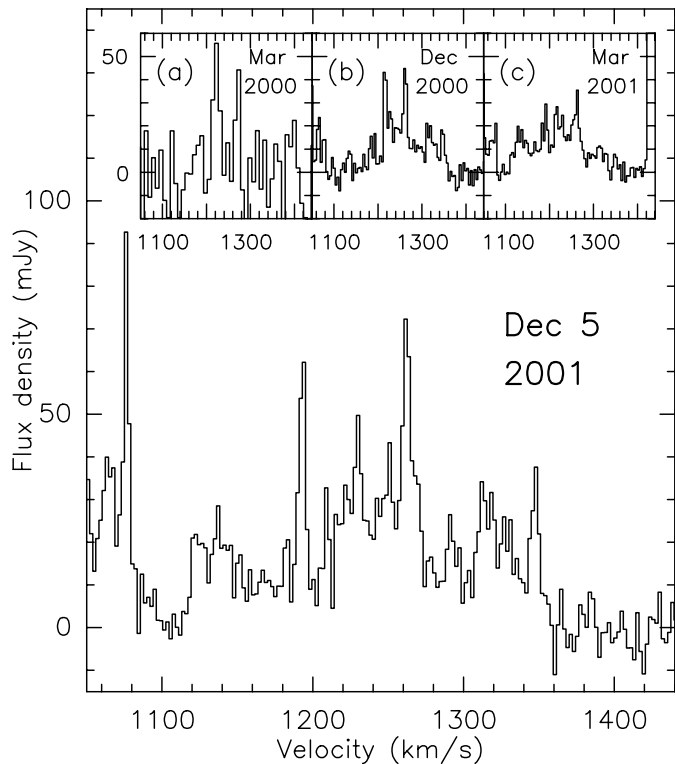


Fig. 2. Near systemic and red-shifted H₂O maser features toward NGC 3079. Channel spacing: 2.1 km s⁻¹ (main spectrum), 4.2 km s⁻¹ (inserts **b** and **c**), and 8.4 km s⁻¹ (insert **a**). The inserted spectra (insert **c**) includes a few bad channels at the edge of the band) show an initially dominant fading 1222 km s⁻¹ component, while the flux of the 1192 km s⁻¹ component increases. The brightest components have an isotropic luminosity of $\sim 0.5 L_{\odot}$. Since the zero level is determined by a linear baseline derived from velocities $V < 920$ and > 1360 km s⁻¹, the absence of H₂O emission near 1100 km s⁻¹ is not entirely certain.

Table 2. Velocities of distinct near systemic or red-shifted features observed on December 5, 2001 (see Fig. 2).

$V(\text{km s}^{-1})$	$V(\text{km s}^{-1})$
1062.7 ± 0.4	1209.3 ± 0.3
1066.8 ± 1.4	1229.8 ± 0.4
1076.5 ± 0.2	1251.1 ± 0.1
1123.0 ± 0.9	1262.1 ± 0.2
1137.7 ± 1.4	1291.5 ± 0.9
1182.6 ± 0.4	1314.4 ± 1.0
1192.9 ± 0.5	1347.6 ± 0.4

Assuming the presence of a symmetric edge-on circumnuclear disk, the systemic velocity of the nuclear region then is ~ 1140 km s⁻¹. Including the 896 km s⁻¹ feature apparent in the early spectra of Henkel et al. (1984) and Haschick & Baan (1985) and tentatively also seen in Dec. 2000 and Dec. 2001, $V_{\text{sys}} \sim 1124$ km s⁻¹. Is this consistent with the systemic velocity of the galaxy?

From the nuclear molecular gas traced by the CO $J = 1-0$ line, Irwin & Sofue (1992) deduced a systemic velocity of $V_{\text{sys}} = 1050 \pm 10$ km s⁻¹. From an H I line profile, Irwin & Seaquist (1991) obtained a midpoint at the 20% peak level of 1123 ± 10 km s⁻¹ and 1126 km s⁻¹ from a fit to the moment map. Three dimensional modeling of their H I data cube yields $V_{\text{sys}} = 1116$ km s⁻¹. The rough agreement of CO, H I, and H₂O velocity centroids implies a nuclear systemic velocity of ~ 1120 km s⁻¹ and suggests that we have seen, for the first time, all the stronger 22 GHz H₂O maser components in NGC 3079. A nuclear systemic velocity of 1230 km s⁻¹ as suggested by Satoh et al. (1999) is not supported by our H₂O data.

Nevertheless, the maser emission is far from perfectly symmetric: (1) All bright components (> 0.5 Jy) are blue-shifted with respect to the systemic velocity which is inconsistent with the situation in NGC 4258 and NGC 1068 as well as with the spiral shock model proposed by Maoz & McKee (1998). (2) The systemic velocity obtained from model fits (Irwin & Seaquist 1991) lies at the edge of that narrow velocity interval ($\Delta V \sim 20$ km s⁻¹, see Fig. 2) that appears to be devoid of H₂O emission (the only such interval over the entire H₂O velocity range observed by us). Interpreted in terms of the paradigm established for NGC 4258, this may hint at a lack of nuclear 22 GHz radio continuum emission at the very center of the putative masering torus. (3) In a well ordered edge-on circumnuclear disk, small line-of-sight velocity gradients that stimulate maser emission should only be present near the tangential points and near the front and back side of the disk. A continuous coverage of the velocity range as observed in NGC 3079 is not expected. (4) None of the four systemic velocities quoted above provides a particularly high number of red- and blue-shifted components that match each other with respect to velocity ($|V_{\text{red}} - V_{\text{sys}}| \sim |V_{\text{blue}} - V_{\text{sys}}|$). Note that the following discussion, does not sensitively depend on the exact choice of V_{sys} as long as it is in the range 1100–1150 km s⁻¹.

Most blue-shifted 22 GHz H₂O velocity components of NGC 3079 are already known to show no significant velocity drift (e.g. Fig. 7 of Nakai et al. 1995; Fig. 6 of Baan & Haschick 1996). The slow drift of ~ 0.4 km s⁻¹ yr⁻¹ suggested by Baan & Haschick (1996) for the 945, 951, and 1015 km s⁻¹ components (V refers to epoch 1994.0) is not expected if a circumnuclear torus is present (e.g. Miyoshi et al. 1995). Our data for the 945 km s⁻¹ component (945.7 and 946.2 km s⁻¹ in Feb. 1994 and 1998, and 946.6 and 946.5 km s⁻¹ in May and June 1998; errors derived from Gaussian fits are ~ 0.3 km s⁻¹) are not contradicting Baan & Haschick (1996), although a group of features with varying amplitudes could also simulate the drift. The 1017 km s⁻¹ component (Fig. 1b) fluctuates between 1014 and 1018 km s⁻¹ and does not support a regular drift, although it is likely related to the 1015 km s⁻¹ component of Baan & Haschick (1996). The 951 km s⁻¹ component was not seen by us. Satoh et al. (1999) and Sawada-Satoh et al. (2000) report a drift of 3.7 ± 0.6 km s⁻¹ yr⁻¹ for a maser feature near 1190 km s⁻¹. We find a group

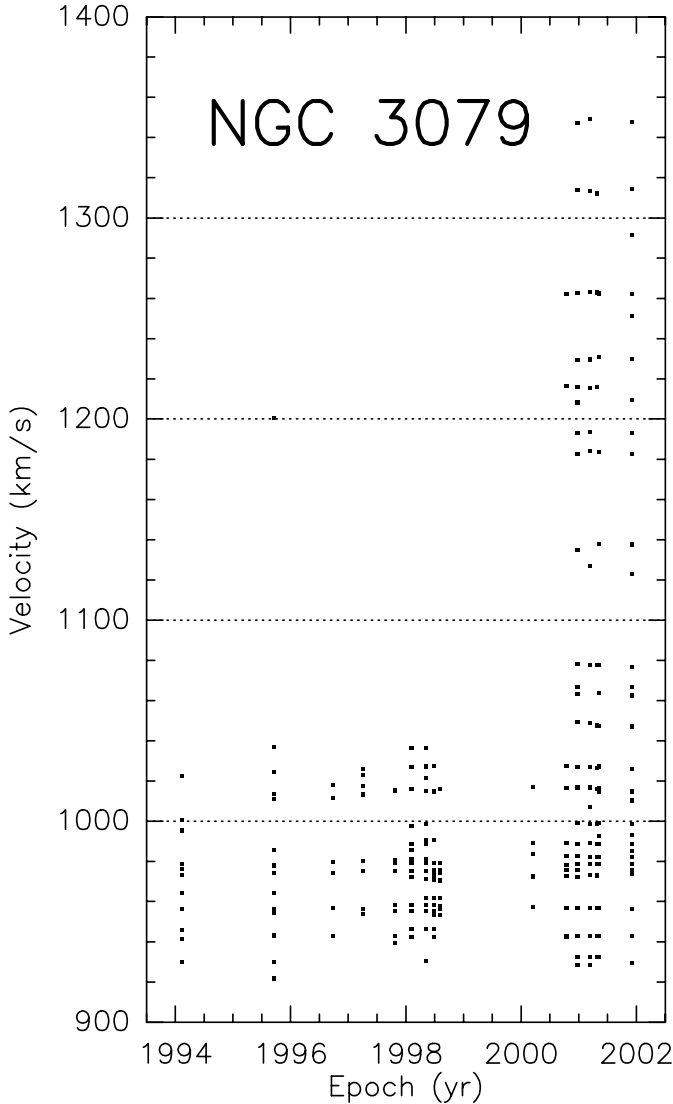


Fig. 3. Individual velocity components of the 22 GHz H₂O spectrum obtained with an accuracy $\lesssim 1 \text{ km s}^{-1}$ for the blue-shifted components and $\sim 1 \text{ km s}^{-1}$ for the redshifted ones.

of features (total width: $V_{\text{tot}} \sim 5\text{--}6 \text{ km s}^{-1}$) centered at 1192.9 km s^{-1} , both on Mar. 3 and Dec. 5, 2001. Thus the drift appears to be well below our estimated detection level of $1.5 \text{ km s}^{-1} \text{ yr}^{-1}$ for a time interval of 9 months. In view of the long lifetime inferred for some of the blue-shifted maser lines (Sect. 3 and Fig. 3), the 1192 km s^{-1} feature reported by Nakai et al. (1995) is likely part of this component, reducing the velocity drift to well below $1.0 \text{ km s}^{-1} \text{ yr}^{-1}$.

The overall lineshape of the H₂O profile is quite distinct from that of NGC 4258 and the morphology of the radio continuum (T. Krichbaum, priv. comm.) is more complex. In spite of the presence of a roughly linear ridge of blue-shifted H₂O masers, the existence of an associated nuclear disk is thus not certain (see e.g. Trotter et al. 1998 for alternative scenarios). Sawada-Satoh et al. (2000) proposed a thick maser disk with continuum source “B” at the nucleus and the 1190 km s^{-1} feature on its near

side (their Fig. 6). Since we see no velocity drift near 1190 km s^{-1} and since this is not the systemic velocity, however, there is no need to put this component at the near side of the putative disk. We therefore tend to favor the disk scenario outlined by Trotter et al. (1998) with the nucleus of the galaxy being located between continuum components A and B (their Fig. 7). In this latter scenario, expected velocity drifts would be consistent with our upper limits. The nucleus would contain a few $10^6 M_{\odot}$ within $R \sim 10 \text{ mas}$ ($\sim 0.7 \text{ pc}$; assumed rotation velocity $V_{\text{rot}} \sim 100\text{--}225 \text{ km s}^{-1}$), the centripetal acceleration and proper motion of the near-systemic components would be difficult to detect ($< 0.1 \text{ km s}^{-1} \text{ yr}^{-1}$ and $\sim 1 \mu\text{as yr}^{-1}$), and most of the red-shifted masers would be located 10–15 mas south of the blue-shifted ones (some masers may be associated with the jet (e.g. Trotter et al. 1998)). Sensitive VLBI data are needed to examine this picture and to obtain definite information on the relative location of blue- and red-shifted maser features and continuum sources in the very center of NGC 3079.

Acknowledgements. We wish to thank M. Inoue and L. J. Greenhill for critically reading the manuscript.

References

- Baan, W. A., & Haschick, A. D. 1996, *ApJ*, 473, 269
 Baars, J. W. M., Genzel, R., Pauliny-Toth, I. I. K., & Witzel, A. 1977, *A&A*, 61, 99
 Gallimore, J. F., Henkel, C., Baum, S. A., et al. 2001, *ApJ*, 556, 694
 Greenhill, L. J., Henkel, C., Becker, R., Wilson, T. L., & Wouterloot, J. G. A. 1995, *A&A*, 304, 21
 Greenhill, L. J., Moran, J. M., & Herrnstein, J. R. 1997, *ApJ*, 481, L23
 Greenhill, L. J. 2000, Proc. of the 5th European VLBI Network Symp., ed. J. E. Conway, A. G. Polatidis, R. S. Booth, & Y. M. Pihlström (Onsala), 101
 Haschick, A. D., & Baan, W. A. 1985, *Nature*, 314, 144
 Haschick, A. D., Baan, W. A., Schneps, M. H., et al. 1990, *ApJ*, 356, 149
 Haschick, A. D., Baan, W. A., & Peng, E. W. 1994, *ApJ*, 437, L35
 Henkel, C., Güsten, R., Downes, D., et al. 1984, *A&A*, 141, L1
 Herrnstein, J. R., Moran, J. M., Greenhill, L. J., et al. 1999, *Nature*, 400, 539
 Irwin, J. A., & Seaquist, E. R. 1991, *ApJ*, 371, 111
 Irwin, J. A., & Sofue, Y. 1992, *ApJ*, 396, L75
 Maoz, E., & McKee, C. F. 1998, *ApJ*, 494, 218
 Miyoshi, M., Moran, J. M., Herrnstein, J., et al. 1995, *Nature*, 373, 127
 Nakai, N., Inoue, M., & Miyoshi, M. 1993, *Nature*, 361, 45
 Nakai, N., Inoue, M., Miyazawa, K., Miyoshi, M., & Hall, P. 1995, *PASJ*, 47, 771
 Ott, M., Witzel, A., Quirrenbach, A., et al. 1994, *A&A*, 284, 331
 Satoh, S., Inoue, M., Nakai, N., et al. 1999, *Adv. Sp. Res.*, 23, 1025
 Sawada-Satoh, S., Inoue, M., Shibata, K. M., et al. 2000, *PASJ*, 52, 421
 Trotter, A. S., Greenhill, L. J., Moran, J. M., et al. 1998, *ApJ*, 495, 740